Magnetic Resonance in Medicine 52:397–402 (2004)

Metabolite and Diffusion Changes in the Rat Brain After Leksell Gamma Knife Irradiation

Vít Herynek,[1*] Martin Burian,[1,2] Daniel Jirák,[1,2] Roman Liščák,[3] Kateřina Náměstková,[2,4,5] Milan Hájek,[1,2] and Eva Syková[2,4,5]

Our study describes the time course of necrotic damage to the rat brain resulting from Leksell Gamma Knife (LGK) irradiation at a dose that was previously considered to be subnecrotic. A lesion induced in the rat hippocampus by 35 Gy irradiation was monitored by MRI, MRS, and DW-MRI for 16 months. T_2-weighted images revealed a large hyperintense area with an increased apparent diffusion coefficient of water (ADC_w), which occurred 8 months after irradiation, accompanied by metabolic changes (increase of lactate (Lac) and choline (Cho), and decrease of creatine (Cr) and N-acetyl aspartate (NAA), as determined by MRS) that indicated an edema. In two animals, the hyperintensity persisted and a postnecrotic cavity connected to enlarged lateral ventricles developed. In the rest of the animals, the hyperintensity started to decrease 9 months post-irradiation (PI), revealing hypointense areas with a decreased ADC_w. Histology confirmed the MRI data, showing either scar formation or the development of a postnecrotic cavity. Magn Reson Med 52:397–402, 2004. © 2004 Wiley-Liss, Inc.

Key words: radiosurgery; MR diffusion; MR spectroscopy; edema; necrosis

The application of subnecrotic doses of gamma irradiation by the Leksell Gamma Knife (LGK) is considered a possible therapy for severe functional disorders, such as intractable epilepsy, in humans (1–5). However, the safety of subnecrotic doses is not strongly supported by experimental data. There is limited information about the long-term impact of LGK irradiation in and around the irradiated area. Previous experimental radiosurgical studies in animals focused on histopathological changes in normal or tumor tissue (6–10). Experimental studies on the anticonvulsive effect of radiosurgery in a rat epilepsy model were recently published (11–13). Chen et al. (11) proved that center doses of 20 or 40 Gy reduced the frequency of seizures, with no signs of necrosis 10 months after irradiation.

In the present study, we aimed to determine whether commonly used doses of irradiation applied to the whole hippocampus could cause undesirable functional or structural impairment (14,15). We studied the time course, evolution, and recovery of diffusion and metabolic changes in the brain after irradiation of the hippocampus by the marginal dose of 35 Gy applied on the 70% isodose. The rats were examined for 16 months after irradiation, the longest observational period yet reported.

MATERIALS AND METHODS

Experiments were performed on 12 male Long-Evans rats (3 months old). Six irradiated rats were followed for 16 months. Four of the rats were repeatedly examined approximately once a month (two rats underwent MRI and MR diffusion measurements during each examination, and two underwent MRI and MRS during each examination). The two remaining rats were examined only once after 16 months, and underwent both MR diffusion and MRS measurements. The results were compared with those obtained in six age-matched control animals.

Radiosurgery

We performed bilateral irradiation of the hippocampus using an LGK. The rats were anesthetized with an intraperitoneal injection of sodium thiopental (Thiopental, VÚAB, Czech Republic) (40 mg/kg) and fixed into a specially designed MRI-compatible stereotactic frame. We then examined the animals by stereotactic MRI using a Siemens Expert 1 T, with a 3D fast low-angle shot (FLASH) T_1-weighted sequence (reconstructed thickness of the slice = 0.8 mm, matrix = 154 × 256, field of view (FOV) = 220 mm). The images were imported to the Leksell GammaPlan treatment planning software, and radiosurgery with the LGK (ELEKTA Instrument AB, Stockholm, Sweden) then followed. We applied a dose of 35 Gy on the 70% isodose to cover the area of the whole hippocampus, using two isocenters of 4 mm collimator for each hemisphere bilaterally. This method is described in detail elsewhere (15). Possible spatial and dose deviations in irradiation were checked with the use of polymer-gel dosimetry (16).

MR Measurement

MR measurements were performed with a 4.7 T Bruker MR spectrometer equipped with an in-house-made surface

[1]MR Unit, Radiology Department, Institute for Clinical and Experimental Medicine, Prague, Czech Republic.

[2]Center for Cell Therapy and Tissue Repair, Prague, Czech Republic.

[3]Stereotactic and Radiation Neurosurgery, Hospital Na Homolce, Prague, Czech Republic.

[4]Institute of Experimental Medicine ASCR, Prague, Czech Republic.

[5]Department of Neuroscience, Charles University, Second Medical Faculty, Prague, Czech Republic.

Grant sponsor: Ministry of Health of the Czech Republic; Grant numbers: IGA MZ NF/5161-3, NF/7411-3, CEZ:L17/98:00023001; Grant sponsor: Ministry of Education, Youth and Sports of the Czech Republic; Grant number: LN00A065.

*Correspondence to: Vít Herynek, MR Unit, Radiology Department, Institute for Clinical and Experimental Medicine, Vídeňská 1958/9, 140 21 Prague 4, Czech Republic. E-mail: vit.herynek@medicon.cz

Received 14 October 2003; revised 5 March 2004; accepted 7 March 2004.

DOI 10.1002/mrm.20150

Published online in Wiley InterScience (www.interscience.wiley.com).

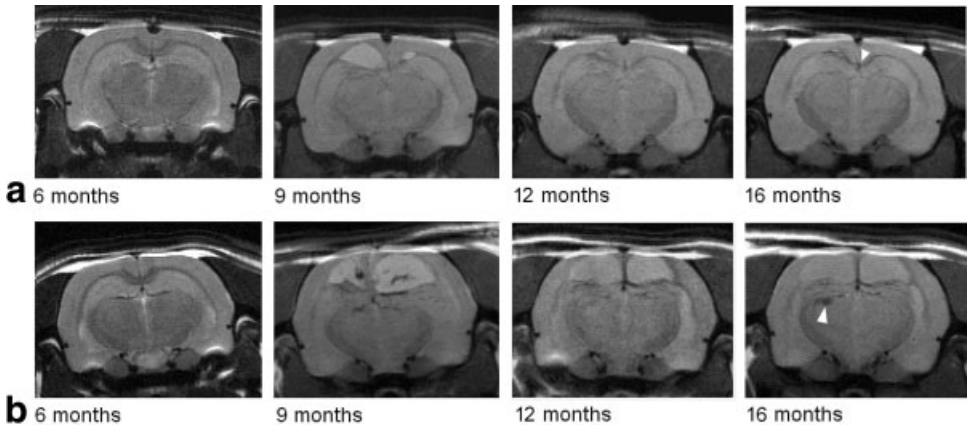

FIG. 1. T_2-weighted MR images of a rat brain, showing the evolution of a lesion 6, 9, 12, and 16 months after irradiation. **a:** An animal that developed a transient lesion. **b:** An animal that developed a post-necrotic cavity. Arrows indicate post-hemorrhagic changes.

head coil. Basic transversal images were acquired with a standard T_2-weighted turbo spin-echo sequence (matrix = 256 × 256, slice thickness = 1 mm, FOV = 4 × 4 cm^2, effective echo time (TE) = 62.7 ms, repetition time (TR) = 3000 ms, turbofactor = 8).

Sets of diffusion-weighted (DW) images were obtained with stimulated-echo acquisition mode (STEAM) sequences (TR = 2000 ms, TE = 38 ms, mixing time (TM) = 11.1 ms, Δ = 30 ms, *b*-values = 19, 58, 135, 404, 826, 1400 s/mm^2, matrix = 128 × 128, FOV = 3.5 × 3.5 cm^2, slice thickness = 1 mm). The diffusion gradient was applied in the anterior–posterior direction. The apparent diffusion coefficient of water (ADC_w) was evaluated by two-parameter fitting. Since there was limited time available for measurement (each measurement obtained under anesthesia represents a certain amount of stress for the animal), and we preferred to measure diffusion more accurately in one direction rather than obtain less accurate results in more directions, we chose to measure the ADC_w value in only one direction.

The spectra were obtained with a single-voxel STEAM sequence, with TE = 3 ms and TR = 5000 ms. The volume of interest was approximately 30 cubic mm for each hemisphere. We evaluated the spectra using LCModel (17) to obtain absolute metabolite concentrations. In this method, a measured spectrum is fitted to a set of spectra (rather than simulated signals) of separate metabolite solutions of known concentration measured in vitro. The parameters of the fit are then easily scaled to the absolute concentrations with the use of additional information, such as voxel size and the transmitter power of the corresponding 90° pulse. The spectra were fitted twice. The first evaluation included fitting to a set of spectra of scyllo-inositol, alanine, aspartate, choline (Cho), creatine (Cr), GABA, glucose, glutamine, glutamate, inositol, lactate (Lac), N-acetyl aspartate (NAA), N-acetyl aspartate glutamate, taurine, and guanosine. Other signals (from macromolecules (MM) and lipids (Lip)) contributed mainly to the baseline. The second evaluation used the same spectral base, but also included the simulation of signals from MM and Lip.

To assess the relaxation time in the chronic lesion, we performed a supplementary T_2 measurement on two controls and two treated animals 14 months after irradiation, using a 30-echo Carr-Purcell-Meiboom-Gill (CPMG) sequence (echo spacing = 8.63 ms, recovery time T_{REC} = 2500 ms). The same geometry was used as for the diffusion measurements. Relaxation maps were evaluated with the use of a program (Chrobak) created by one of the current authors (V. Herynek). We evaluated T_2 values for each pixel using a three-parameter fit with a variable number of points (to avoid fitting points with a too-low signal-to-noise ratio (SNR)). To avoid an error caused by imperfect pulses (CPMG compensates only even echoes), we used only even echoes for the T_2 evaluation.

The animals were anesthetized during all of the MR experiments. They spontaneously breathed a mixture of isofluranum (Forane®; Abbott, Czech Republic) in air at concentrations of 3% and 1.5–2% for induction and maintenance, respectively. Each examination lasted 2–3 hr.

Histology

Six irradiated animals and two control animals were used for histological examinations. The animals were killed 17 months after irradiation with a barbiturate overdose (200 mg/kg). They were transcardially perfused with buffered saline, followed by 4% buffered formaldehyde. Every fourth brain section (40 μm thick) was stained with cresyl violet to visualize the extent of the changes induced by irradiation. Additional slices were stained with luxol fast blue. The slices were observed on an Axioskop 2, and photographs were taken with an Axiovision set (Carl Zeiss, Germany).

Statistical Evaluation

We used an analysis of variance (ANOVA) for a statistical comparison of the treated animals and controls. Since the data sets were small and unbalanced, we used the Scheffé method.

All animal experiments were carried out in accordance with the European Communities Council Directive of 24 November 1986 (86/609/EEC).

RESULTS

The first diffusion changes occurred in the irradiated rats at the same time, during the 6th month post-irradiation (PI). The changes in the T_2-weighted images became visible as a hyperintense area that occurred 8 months PI, and

the hyperintense area reached its maximal size during the 9th month PI. Subsequently, the evolution of the lesion varied among different animals (see Fig. 1). In two rats the hyperintense area disappeared after 12 months PI (Fig. 1a), revealing a small area with a hypointense signal in T_2-weighted images, whereas in two other animals the signal remained hyperintense in the T_2-weighted images (Fig. 1b), suggesting the development of a cavity filled with cerebrospinal fluid in the irradiated area of the brain. Small hypointense areas in the thalamus and the medial part of the corpus callosum occurred in the case of two animals 16 months PI (Fig. 1a and b).

MR Diffusion

The control animals revealed no substantial changes in the ADC_w during the entire period of measurement. The average value of ADC_w (D) in the hippocampus measured in the posterior–anterior direction was 775 ± 28 $\mu m^2 s^{-1}$. No significant changes in ADC_w were found in LGK-treated animals during the first 6 months PI (D = 816 ± 32 $\mu m^2 s^{-1}$). A mild increase in the ADC_w in the hippocampus occurred 6 months PI (D = 898 ± 78 $\mu m^2 s^{-1}$, $P < 0.03$), although no change was seen in T_2-weighted images (see Fig. 1). Eight months after irradiation, a T_2 hyperintensity was observed, which reached its maximum approximately 1 month later. The ADC_w increased to very high values in both the cortex (over D > 2000 $\mu m^2 s^{-1}$) and the hippocampus (over D > 1400 $\mu m^2 s^{-1}$). Ten months PI, ADC_w in the compressed tissue of the hippocampus below the necrotic cavity dropped and remained significantly lower (D < 700 $\mu m^2 s^{-1}$) compared to controls (see Fig. 2a). In two animals 10 months PI, the hyperintensity in the cortex diminished, and the ADC_w returned to normal values (see Fig. 2b). In half of the animals, an extensive lesion persisted for 16 months with high diffusion values and high T_2 relaxation times (210 ± 60 ms) in the respective part of the cortex. The mean T_2 value observed in the control animals was T_2 = 57.0 ± 0.6 ms, and the relaxation time in the case of the animals with diminished hyperintensity was T_2 = 56.9 ± 1.7 ms.

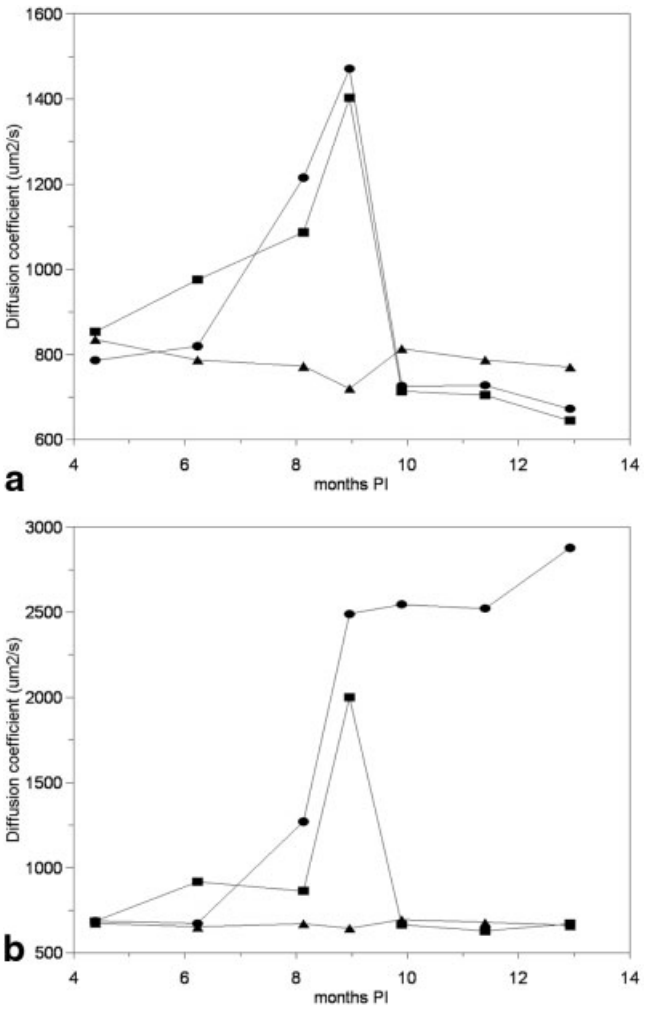

FIG. 2. Evolution of ADC_w values in the rat brain 4–16 months after LGK irradiation. **a:** Hippocampus. **b:** Cortex. ●: Rat with a permanent lesion. ■: Rat with a transient lesion. ▲: Control.

MR Spectroscopy (MRS)

MRS evaluation, which also included fitting to simulated signals of MM and Lip, proved that these compounds were present in the spectra (Fig. 3), particularly when an edema occurred. However, the results of this evaluation are very unreliable and do not provide consistent metabolite concentrations, due to the overlapping of metabolite signals with the Lip and MM contributions. More consistent results were obtained when we omitted the fitting of MM and Lip, which we included in the spectral baseline. Table 1 summarizes the results obtained by this method.

In agreement with the diffusion measurements, we observed no metabolic changes during the first 6 months after irradiation. Spectroscopy revealed a significant increase ($P < 0.01$) of Cho and a decrease ($P < 0.01$) of Cr 8 months PI (see Table 1). When hyperintensity occurred in T_2W images, an increase of the signal at 1.3 ppm attributed to Lac was found (Fig. 3d). The signal at 2.0 ppm (attributed to NAA) did not change significantly (see Table 1). Since signals at 0.9 and 0.6 ppm attributed to Lip occurred at the same time, we have to consider the possibility that lipid signals contributed to the signals at 1.3 and even 2.0 ppm. Nevertheless, we were not able to quantify the possible contribution of the Lip signal to the Lac and NAA signals. The concentrations of Cr and Cho began to recover to normal values as the hyperintensity disappeared. NAA began to change 12 months PI. The concentration later decreased to approximately 60% of normal values. The Lac signal decreased back to normal values.

In the case of the animals with a formed cavity, we observed lower concentrations of Cr, Cho, and NAA compared to controls. The Lac signal decreased close to normal values in both hemispheres (Fig. 3f).

Histology

The histological results were consistent with the MRI observations. Four animals showed minor tissue damage that did not result in a cavity, and two animals developed a postnecrotic cavity.

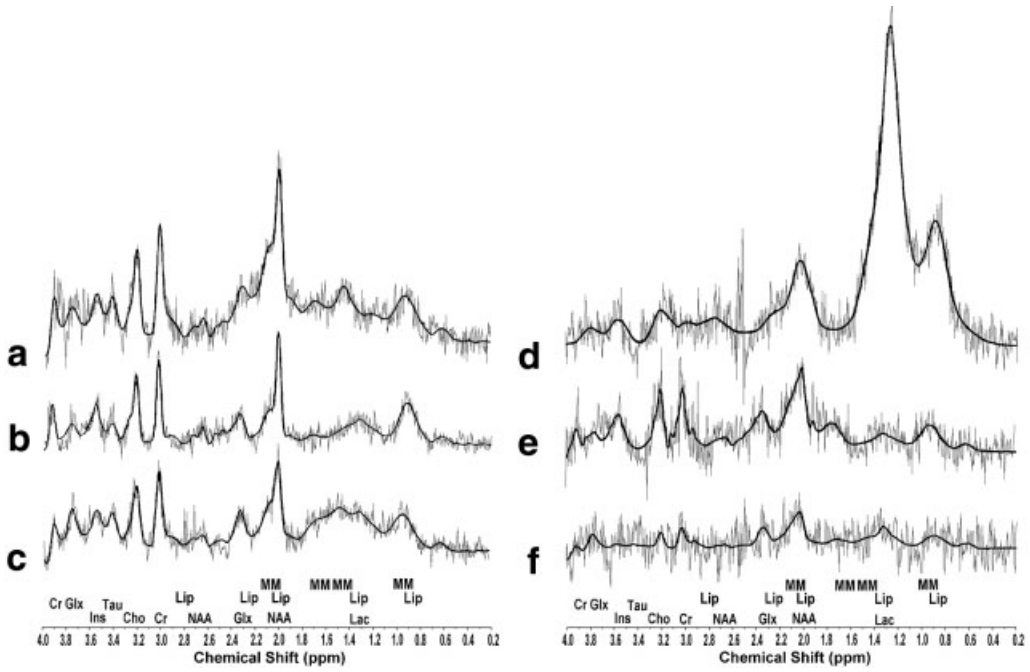

FIG. 3. MR spectra from the rat hippocampus. **a:** Spectrum of a control rat. **b:** Spectrum of a rat 1 month PI. **c:** 7 months PI. **d:** 9 months PI, when the lesion developed. **e:** Spectrum from a rat in which a cavity did not develop, obtained 14 months PI. **f:** Spectrum from a rat with a developed cavity 14 months PI. The solid line in the figures represents a calculated fit to the spectra.

In the four animals in which tissue damage did not result in a cavity, we detected severe damage to the white matter (Fig. 4a): the thickness of the corpus callosum was reduced to a thin layer of densely packed nuclei (Fig. 5d–f). There were signs of hemorrhage in the medial part of the corpus callosum. The thickness of the alveolus and stratum oriens in the hippocampus was also reduced. The cortical layers remained organized, while the lateral ventricles were dilated.

The two animals in which T_2-weighted images revealed hyperintensity throughout the observation period showed extensive changes (Fig. 4b). The region of the corpus callosum and the adjacent cortex were transformed into a cavity connected to the dilated lateral ventricles. Partial necrosis extended to the alveus hippocampi and the stratum oriens. The CA1 pyramidal cell layer lost more than half of its cell layers compared to controls. The hippocampal structure was retracted toward the cavity, but the layered organization was not completely disrupted. Extensive changes were also found in the somatosensory cortex. The necrosis extended to the whole cortical width in some sections, whereas in other sections the cortical layers remained organized despite a severe reduction in cortical thickness.

DISCUSSION

Our results show that the first signs of necrotic damage were visible in diffusion maps as early as 6 months after irradiation. The changes became visible on T_2-weighted

Table 1
Absolute Concentrations (in mM) of Selected Metabolites (Cho-Choline Compounds, Cr-Creatine/Phosphocreatine, NAA - N-acetyl aspartate, Lac - Lactate) in the Hippocampus After Irradiation

	Cho (mM)	Cr (mM)	Lac (mM)	NAA (mM)
Controls, $N = 4$	2.1 ± 0.3	8.9 ± 1.9	1.8 ± 2.2	9.8 ± 1.5
<6 months, $N = 2$	1.9 ± 0.2	8.3 ± 0.6	1.2 ± 1.3	8.4 ± 1.0
6 months, $N = 2$	2.1 ± 0.5	8.3 ± 0.6	2.4 ± 0.7	11.0 ± 3.9
8 months, $N = 2$	3.1 ± 0.7	5.1 ± 1.4	37.5 ± 30.5[c]	11.6 ± 2.4[c]
9 months, $N = 2$	3.0 ± 0.3	6.3 ± 1.4	22.5 ± 12.4[c]	9.7 ± 1.7[c]
12 months, $N = 2$	1.7 ± 0.1	5.4 ± 0.5	7.3 ± 1.2[c]	7.9 ± 1.6[c]
14–16 months, $N = 3$[a]	2.4 ± 1.0	7.1 ± 2.3	3.5 ± 1.1[c]	6.1 ± 2.1[c]
14–16 months, $N = 1$[b]	0.7 ± 0.3	1.9 ± 0.9	4.9 ± 1.2[c]	4.8 ± 0.8[c]

[a]Animals without a developed postnecrotic cavity.
[b]An animal with a cavity.
[c]The lactate and NAA signals might be overlapped by the signals of lipids, and the numbers represent virtual concentrations as if the signals represent pure lactate or NAA, respectively.
N, no. of animals measured.

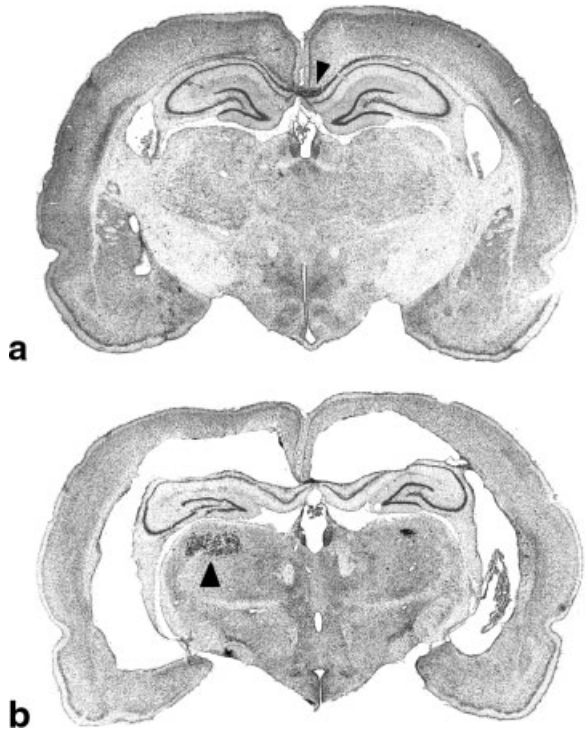

FIG. 4. Cresyl violet staining of a coronal brain section from an irradiated animal 17 months PI. **a:** An animal in which hyperintensity on MRI was transient. The thickness of the corpus callosum is severely reduced, the lateral ventricles are dilated, and the hippocampal structure shows retraction. An arrow indicates the hemorrhage. **b:** Coronal brain section of an irradiated animal in which a postnecrotic cavity developed. Severe necrotic damage in the area of the corpus callosum, the adjacent cortex, and the stratum oriens hippocampi is apparent. Hemorrhage is visible in the thalamus (indicated by an arrow). The lateral ventricles are dilated and connected to the postnecrotic cavity.

images 8 months PI, together with metabolite changes observed by MRS. The observed hyperintense areas on the T_2-weighted images were a sign of a cytotoxic edema. Of course, MRI cannot distinguish between cytotoxic and vasogenic edemas. However, a vasogenic edema usually turns into a cytotoxic edema after several days. Therefore, we concluded that an edema we observed for several months was, in fact, cytotoxic.

The edema led to severe necrotic damage and, in some animals, to the creation of a postnecrotic cavity in the cortex and hippocampus. This was reflected by an increased ADC_w (Fig. 2). Although the focal point of the irradiation was the dorsal hippocampus, it is clear that the cortex was irradiated as well. Our previous observations in pilot studies with different irradiation planes (14,15) showed that the cortical area is more susceptible to damage after irradiation. The deep cortical layers were damaged and necrotic, whereas the hippocampus was atrophied and retracted from the cavity but retained its layered organization. The reason for such differences is not known, but the hippocampus is a highly plastic region with the ability to give rise to new neurons even in adulthood.

We observed an increase in Lip and Lac signals, and a decrease of Cr in the edematous tissue, where blood circulation and metabolism were impaired. The subsequent partial decrease in Lac/Lip signals (approximately 12 months PI) can be explained by the release of pressure that occurred after the cytotoxic edema and lesion regressed, followed by lower Lac production. A decrease in the signal at 2.0 ppm assigned to NAA was observed 12 months PI (4 months after the first signs of the lesion were visible). The decrease of NAA 12 months PI is a sign of cellular loss in the lesion. However, the NAA concentration might have been reduced even earlier, but concealed by an overlap with the lipid signal. Lipid signals are present in the spectra when an edema occurs (they are identified at 0.9 and 0.6 ppm (see Fig. 3d)); therefore, we deduce that they also contribute to signals at 1.3 and 2.0 ppm. The convolution of a Lip signal at 2.0 ppm with the signal of NAA might cause an insignificant increase in the signal at 2.0 ppm (see Table 1), and cover up a moderate decrease in NAA concentration (caused by cellular loss in the lesion) at an early stage of the edema. This explanation is supported by the broadening of the signal at 2.0 ppm, and

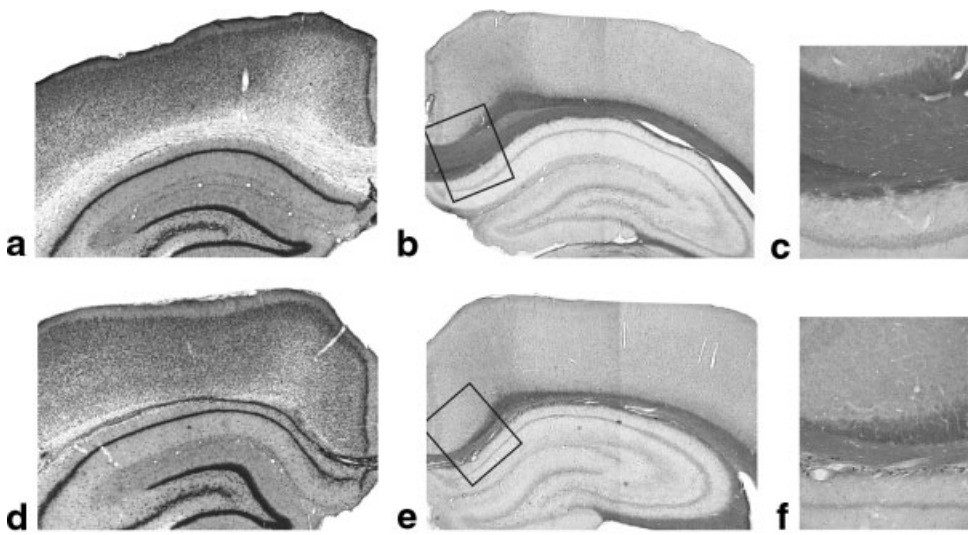

FIG. 5. Coronal sections of a rat brain stained with cresyl violet and luxol fast blue. **a:** Left hemisphere of a control animal. **b:** Right hemisphere of the same animal stained with luxol fast blue. **c:** An enlarged area of the corpus callosum (the area is marked in **b**). **d:** Left hemisphere of an animal with transient hyperintensity on MRI 17 months PI, stained with cresyl violet. **e:** Right hemisphere of the same animal stained with luxol fast blue. **f:** An enlarged area of the corpus callosum (the area is marked in **e**). The reduction in the thickness of the corpus callosum, and cysts in the adjacent tissue of the irradiated animal are both obvious.

corresponds well with previous results obtained in humans (19). Also, the signal at 1.3 ppm (attributed to Lac) is a convolution of the Lac and Lip signals. We were unable to reliably quantify the Lip concentration, as that would have required more sophisticated measurement and evaluation methods, including outer volume suppression, metabolite nulling, and adequate prior knowledge of the spectra (20).

Histological examination confirmed the severe damage visible on the MR images. In four animals, irradiation caused damage to the corpus callosum, and a loss of cells in layers of the somatosensory cortex and the striatum oriens hippocampi. In another two animals, necrotic damage led to the development of hydrocephalus and a postnecrotic cavity filled with cerebrospinal fluid. The presence of a postnecrotic cavity with residual metabolites in the vicinity of the edema corresponds to the NAA decrease found by MRS, and the high ADC_w values observed in the lesion 12 months or more after irradiation.

The hypointense areas observed inside the edematous necrotic tissue, in the medial part of the corpus callosum (Fig. 1a) and the thalamus (see Fig 1b), were confirmed by histology as post-hemorrhagic changes (see Fig. 4a and b).

The long-term response to irradiation demonstrates that the application of a marginal irradiation dose of 35 Gy leads to damage of the corpus callosum and the somatosensory cortex, in addition to the hippocampus. The volume of irradiated tissue was larger than that observed in previous studies (7,9,11–13,18), and the delayed effect of the radiation on compromising the cerebral microcirculation exceeded a tolerable volume. Thus, a small variability in isodose volumes caused by the individual treatment plans for each animal could have been responsible for the observed inconsistency. The focal point for irradiation was focused on a whole-body 1 T imager that did not have sufficient resolution for small animals, so we can not rule out the possibility that neighboring structures in the rat brain were partially irradiated. The displacement of the distribution profile center during irradiation assessed by gel-dosimetry (16) reached 0.6 mm, and the volume covered by the 70% isodose therefore varied between 184 and 212 mm^3.

CONCLUSIONS

We observed and quantified the evolution of diffusion and metabolic changes in the rat brain after irradiation by the LGK. The first signs of a cytotoxic edema accompanying necrotic changes were visible 6 months after irradiation by a marginal dose of 35 Gy using four isocenters of 4 mm collimator. Three months later, MRS revealed the start of further cell death. Twelve months after irradiation, a regression of the lesion was observed, but in some cases an extensive water-filled cavity developed. In all of the animals, severe damage to the corpus callosum was revealed by histology 17 months after irradiation, and in 50% of the animals hydrocephalus developed with severe damage to the cortex and hippocampus. The applied dose cannot be considered to be subnecrotic, as it caused severe functional and structural impairment.

REFERENCES

1. Alexander III E, Lindquist C. Special indications: radiosurgery for functional neurosurgery and epilepsy. In: Alexander III E, Loeffler JS, Lunsford LD, editors. Stereotactic radiosurgery. New York: McGraw-Hill; 1993. p 221–225.
2. Barcia-Salorio JL, Barcia JA. The role of radiosurgery in the treatment of epilepsy. In: Gildenberg PL, Tasker RR, editors. Textbook of stereotactic and functional neurosurgery. New York: McGraw-Hill; 1998. p 1925–1932.
3. Heikkinen ER, Heikkinen MI, Sotaniemi K. Stereotactic radiotherapy instead of conventional epilepsy surgery: a case report. Acta Neurochir (Wien) 1992;119:159–160.
4. Regis J, Peragui JC, Rey M, Samson Y, Levrier O, Porcheron D, Regis H, Sedan R. First selective amygdalohippocampal radiosurgery for mesial temporal lobe epilepsy. Stereotact Funct Neurosurg 1995;64(suppl 1): 193–201.
5. Whang CJ, Kwon Y. Long-term follow-up of stereotactic gamma knife radiosurgery in epilepsy. Stereotact Funct Neurosurg 1996;66(suppl 1):349–356.
6. Altschuler E, Lunsford LD, Kondziolka D, Wu A, Maitz AH, Sclabassi R, Martinez AJ, Flickinger JC. Radiobiologic models for radiosurgery. Neurosurg Clin N Am 1992;3:61–77.
7. Kamiryo T, Kassell NF, Thai QA, Lopes MB, Lee KS, Steiner L. Histological changes in the normal rat brain after gamma irradiation. Acta Neurochir (Wien) 1996;138:451–459.
8. Kamiryo T, Lopes MBS, Berr SS, Lee KS, Kassell NF, Steiner L. Occlusion of the anterior cerebral artery after gamma knife irradiation in a rat. Acta Neurochir (Wien) 1996;138:983–991.
9. Kondziolka D, Lunsford LD, Claassen D, Maitz A, Flickinger JC. Radiobiology of radiosurgery: part I. The normal rat brain model. Neurosurgery 1992;31:271–279.
10. Marks LB, Spencer DP, Acker JC, Yang W, Avery MA, Dodge RK, Dewhirst MW. Radiosurgery in rat brain. In: Kondziolka D, editor. Radiosurgery. Vol. I. Basel: Karger; 1996. p 308–315.
11. Chen Z, Kamiryo T, Henson SL, Yamamoto H, Bertram EH, Schottler F, Patel F, Steiner L, Prasad D, Kassell NF, Shareghis S, Lee KS. Anticonvulsant effects of gamma surgery in a model of chronic spontaneous limbic epilepsy in rats. J Neurosurg 2001;94:270–280.
12. Maesawa S, Kondziolka D, Dixon CE, Balzer J, Fellows W, Lunsford LD. Subnecrotic stereotactic radiosurgery controlling epilepsy produced by kainic acid injection in rats. J Neurosurg 2000;93:1033–1040.
13. Mori Y, Kondziolka D, Balzer J, Fellows W, Flickinger JC, Lunsford LD, Thulborn KR. Effects of stereotactic radiosurgery on an animal model of hippocampal epilepsy. Neurosurgery 2000;46:157–168.
14. Náměstková K, Liščák R, Herynek V, Burian M, Jirák D, Hájek M, Brožek G, Mareš V, Syková E. In: Book of Abstracts, 4th Conference of the Czech Neuroscience Society, Prague, 2001.
15. Liscak R, Vladyka V, Novotny Jr J, Brozek G, Namestkova K, Mares V, Herynek V, Jirak D, Hajek M, Sykova E. Leksell Gamma Knife lesioning of the rat hippocampus: the relationship between radiation dose and functional and structural damage. J Neurosurg 2002;97(5 Suppl):666–673.
16. Novotny J, Dvorak P, Spevacek V, Tintera J, Novotny J, Cechak T, Liscak R. Quality control of the stereotactic radiosurgery procedure with the polymer-gel dosimetry. Radiother Oncol 2002;63:223–230.
17. Provencher SW. Estimation of metabolite concentrations from localized in vivo proton NMR spectra. Magn Reson Med 1993;30:672–679.
18. Kamiryo T, Lopes MB, Kassell NF, Steiner L, Lee KS. Radiosurgery-induced microvascular alterations precede necrosis of the brain neuropil. Neurosurgery 2001;49:409–414.
19. Hajek M, Dezortova M, Liscak R, Vymazal J, Vladyka V. 1H MR spectroscopy of mesial temporal lobe epilepsies treated with Gamma knife. Eur Radiol 2003 May;13:994–1000.
20. Seeger U, Klose U, Mader I, Grodd W, Nägele T. Parameterized evaluation of macromolecules and lipids in proton MR spectroscopy of brain diseases. Magn Reson Med 2003;49:19–28.